

# Surface electronic band structure and $\bar{A}$ surface state lifetimes at the Be(10 $\bar{1}0$ ) surface: Experiment and theory

T. Balasubramanian,<sup>1</sup> L. I. Johansson,<sup>2</sup> P. -A. Glans,<sup>2</sup> and C. Virojanadara,<sup>2</sup> V. M. Silkin,<sup>3</sup> E. V. Chulkov,<sup>3,4</sup> and P. M. Echenique<sup>3,4</sup>

<sup>1</sup>*MAX-Lab, Lund University, S 22100, Lund, Sweden*

<sup>2</sup>*Department of Physics, Linköping University, S 58183, Linköping, Sweden*

<sup>3</sup>*Donostia International Physics Center (DIPC), 20018 San Sebastián/Donostia, Basque Country, Spain*

<sup>4</sup>*Departamento de Física de Materiales and Centro Mixto CSIC-UPV/EHU, Facultad de Ciencias Químicas, Universidad del País Vasco/Euskal Herriko Unibertsitatea, Apdo. 1072, 20018 San Sebastián/Donostia, Basque Country, Spain*

(Received 3 November 2000; revised manuscript received 29 March 2001; published 18 October 2001)

The surface electronic band structure of the Be(10 $\bar{1}0$ ) surface is experimentally determined by angle-resolved photoemission and calculated by using density-functional theory. The experimental results agree well with the calculations, except for the fact that we were only able to resolve three surface states in the gap at  $\bar{L}$ , instead of four as predicted by the calculations. Through the temperature-dependent study, the phonon contribution subtracted width ( $\hbar$  times inverse lifetime) of the shallow surface state at  $\bar{A}$  is found to be  $51 \pm 8$  meV. This is compared with the electron-electron interaction contribution to the width (53 meV) of the shallow surface state at  $\bar{A}$  obtained from model potential calculations.

DOI: 10.1103/PhysRevB.64.205401

PACS number(s): 73.20.At, 79.60.Bm

## I. INTRODUCTION

There has been a continued interest both experimentally and theoretically in studying the surfaces of Be.<sup>1-21</sup> Bulk Be is a semimetal with very low electron density of states (DOS) at the Fermi level,  $E_F$ . However, the two low index surfaces, namely, the (0001) and the (10 $\bar{1}0$ ) have surface DOS at  $E_F$  about 3–4 times larger than their bulk DOS at  $E_F$  making the surfaces metallic. This is due to the large number of surface states that exist at these two surfaces.<sup>1-7</sup> Many of the interesting properties observed at these two surfaces are closely linked to the existence of these surface states. Some examples are large Friedel oscillations,<sup>9,10</sup> large surface core-level shifts,<sup>11-15</sup> and an enhanced electron-phonon mass enhancement parameter at the surface compared to bulk.<sup>16-20</sup> A complete mapping of all the surface states is thus important. For Be(0001), the mapping of the surface electronic states by angle-resolved photoemission spectroscopy (ARPES) (Refs. 1 and 2) is in good agreement with the theoretical calculations.<sup>3-5</sup> However, for Be(10 $\bar{1}0$ ) this is not the case. The Be(10 $\bar{1}0$ ) surface can have two terminations, short and long. The surface electronic structure of these two terminations are different.<sup>6,7</sup> The results of an earlier ARPES experiment clearly indicated that the short termination is preferred to the long.<sup>7</sup> The previous theoretical study predicted six occupied surface states<sup>6,7</sup> and out of these four were observed and two surface states at the  $\bar{L}$  point were not observed.<sup>7</sup> Unoccupied states with an impact on image-potential states have also been recently investigated theoretically at the  $\bar{\Gamma}$  point.<sup>21</sup>

In this paper we report ARPES experimental mapping of the surface electronic band structure of Be(10 $\bar{1}0$ ) along with improved calculations of these states. We also study here the electron-electron and the electron-phonon contributions to the inverse lifetime (linewidth),  $\tau^{-1}$ , of the shallow surface

state at the  $\bar{A}$  point (there are two occupied surface states at  $\bar{A}$ ; we use the nomenclature shallow for the surface state close to  $E_F$ ). This surface state was chosen as it is the most interesting state owing to the fact that it is localized mainly in the surface layer, crosses the Fermi level, and determines high DOS at  $E_F$  on Be(10 $\bar{1}0$ ).<sup>6,7</sup> We report a model potential calculation of the electron-electron contribution to  $\tau^{-1}$  and experimentally determine the electron-phonon contribution from a temperature-dependent study of the surface state. By subtracting the electron-phonon contribution from the total width we obtain the electron-electron plus the electron-impurity interaction contribution to the hole lifetime and compare it with the calculated result.

This paper is organized as follows. In Sec. II, details of the experimental setup are presented. In Sec. III, we present the calculation method for the surface band structure. The ARPES determination of the surface band structure is presented in Sec. IV. The results of the calculations are presented in Sec. V. Apart from the surface band structure along  $\bar{\Gamma}$ - $\bar{M}$ ,  $\bar{\Gamma}$ - $\bar{A}$ ,  $\bar{A}$ - $\bar{L}$ , and  $\bar{L}$ - $\bar{M}$ , the present calculations also include the surface states along the  $\bar{\Gamma}$ - $\bar{L}$  direction. The main difference between the results of the earlier and the present calculations are (1) there are four surface states at  $\bar{L}$  instead of two as reported by the earlier calculations, and (2) there are two surface states at  $\bar{M}$  instead of one as predicted earlier. Apart from the fact that we were able to resolve experimentally only three surface states at  $\bar{L}$ , the measured results agree well with the calculations. In Sec. VI, we present model potential calculations of the electron-electron contribution to the lifetime of the shallow surface state at  $\bar{A}$ . The calculations give the electron-electron contribution to be 53 meV. Experimental determination of the electron-phonon and the electron-electron plus electron-impurity contribution to the lifetime through a temperature-dependent study of the

width of the surface state at  $\bar{A}$  is presented in Sec. VII. The zero-temperature extrapolated electron-phonon contribution is 84 meV, the electron-electron plus the electron-impurity contribution is  $51 \pm 8$  meV. Finally the conclusions are presented in Sec. VIII.

## II. EXPERIMENTAL DETAILS

The experiments were performed at beamline 33, at the MAX-I synchrotron-radiation facility in Lund, Sweden. The beamline is equipped with a spherical grating monochromator (SGM)<sup>22</sup> and a Vacuum Generators (VG) end station equipped with a variable angular resolution VG 75-mm electron analyzer.<sup>23</sup> The incident angle was set to  $45^\circ$  in the horizontal plane. The angular resolution unless otherwise specified was set to  $\pm 2^\circ$ . The total-energy resolution of the photons plus the analyzer varied between 60 and 100 meV for photon energy in the range of 21.2 eV to 70 eV. The Be(10 $\bar{1}$ 0) single crystal was mounted on a 0.2-mm tungsten wire. This wire was also used for heating the crystal. The crystal was cleaned by repeated Ne<sup>+</sup> sputter and anneal cycles. For the temperature-dependence study, the heating current was pulsed at 1 kHz with a 20% duty cycle and the electron counting was disabled when the heating current was on. During the temperature-dependent studies, the temperature of the sample was stable to within 5 °C. The surface order was checked with low-energy electron diffraction (LEED) which showed a rectangular  $1 \times 1$  pattern typical of the Be(10 $\bar{1}$ 0) surface.

For determining the surface states and their dispersions along  $\bar{\Gamma}-\bar{A}$ ,  $\bar{\Gamma}-\bar{M}$ , or  $\bar{\Gamma}-\bar{L}$ , the sample was oriented with LEED such that the direction scanned is in the horizontal plane. For determining the surface states and their dispersions along  $\bar{A}-\bar{L}$  ( $\bar{M}-\bar{L}$ ), the sample was first oriented such that  $\bar{\Gamma}-\bar{M}$  ( $\bar{\Gamma}-\bar{A}$ ) was in the horizontal plane. The analyzer was then moved to  $\bar{A}$  ( $\bar{M}$ ) corresponding to the state under investigation and the dispersion along  $\bar{A}-\bar{L}$  ( $\bar{M}-\bar{L}$ ) was determined by moving the analyzer in the horizontal plane. All the spectra for mapping of the surface band structure were taken at room temperature.

## III. CALCULATION METHOD

Our first-principles calculations are based on density-functional theory with the local-density approximation for exchange and correlation.<sup>24</sup> A model of thin films periodically repeated in the direction perpendicular to the surface and separated by vacuum intervals is employed. The (10 $\bar{1}$ 0) surface of hcp metals can be terminated with either short or long first interlayer spacing. Clear preference for the short first interlayer spacing termination of Be(10 $\bar{1}$ 0) has been found both experimentally and theoretically.<sup>7,8</sup> Therefore this surface geometry is used in the present study. Calculations have been performed with the use of films consisting of 24 atomic layers and separated by vacuum intervals corresponding to 12 atomic layers. For two outer atomic layer spacings on each side of the slabs we use the relaxed atomic plane

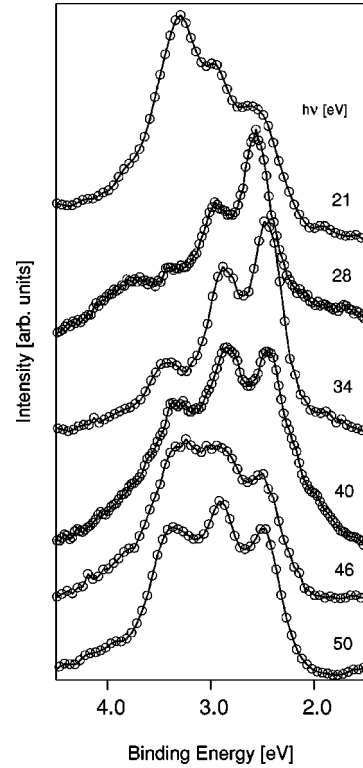


FIG. 1. Series of spectra at the  $\bar{L}$  point at various photon energies. The open circles are the experimental points and the lines are to guide the eye. The photon energy of each spectrum is also indicated.

positions, obtained in Ref. 21. In that geometry the first interlayer spacing is contracted by 19% and the second one is expanded by 8%, which is in good agreement with experimental and other theoretical results for corresponding interlayer spacings.<sup>7,8</sup> The norm-conserving nonlocal ion pseudopotential of Be was generated according to Refs. 25 and 26. The electron wave functions were expanded in a set of plane waves up to a kinetic-energy cutoff of 16 Ry. This basis provides the convergence of calculated one-electron energies better than 0.1 eV. The Brillouin-zone (BZ) integrations were performed with the use of a 64-point grid in the irreducible quarter of the surface BZ.

## IV. SURFACE ELECTRONIC BAND STRUCTURE: EXPERIMENT

Photon energy scans at all surface BZ symmetry points were performed to determine the surface states. One such set of spectra taken at the  $\bar{L}$  point is shown in Fig. 1. In contrast to the previous experimental study<sup>7</sup> three states are clearly seen in Fig. 1 and furthermore the binding energy of these states does not change with photon energy. The binding energies of these three states at the  $\bar{L}$  point are 2.45 eV, 2.8 eV, and 3.4 eV. These states are also sensitive to contamination and fall in the theoretically calculated bulk band gap that has a bottom at 3.6 eV.

Angular scans were done along all symmetry directions to determine the surface band structure. The scans were done at  $\hbar\nu = 22$  eV, 26 eV, 30 eV, 34 eV, 38 eV, 60 eV, and 70 eV.

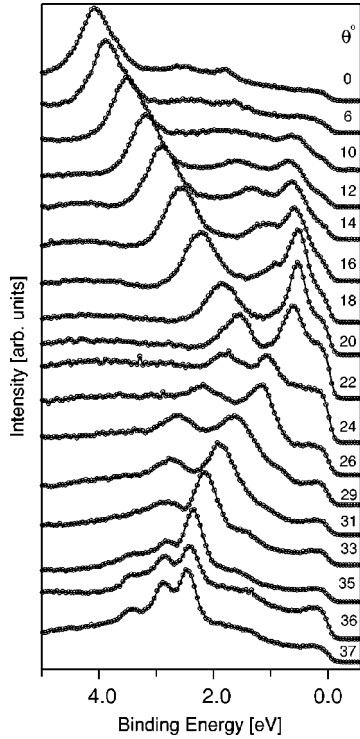


FIG. 2. Room-temperature spectra at various angles along the  $\bar{\Gamma}$ - $\bar{L}$  direction. The photon energy is 34 eV. The open circles are the experimental points and the lines are to guide the eye. The energy resolution is 80 meV and the angular resolution is  $\pm 2^\circ$ . The sample was oriented such that the  $\bar{\Gamma}$ - $\bar{L}$  direction is in the horizontal plane. The angles with respect to the sample normal is indicated in each spectrum.

A typical set of spectra of angular scans along  $\bar{\Gamma}$ - $\bar{L}$  taken with a photon energy of 34 eV and with energy and angular resolution of 80 meV and  $\pm 2^\circ$ , respectively, is shown in Fig. 2. In Fig. 1 and Fig. 2 one can notice small peaks above the uppermost surface state at the  $\bar{L}$  point. These peaks do not disperse much with  $\mathbf{k}_\parallel$ . We believe that these small peaks are related to impurities/defects in the sample band structure. In

Table I, we present the binding energy of the surface states from experiments and from the calculations at all the symmetry points and at the midpoint along the  $\bar{\Gamma}$ - $\bar{L}$  direction. The main difference between the experimentally determined and the calculated surface band structures is that we were able to resolve only three surface states at  $\bar{L}$  instead of four with binding energies of 2.4 eV, 2.8 eV, 3.4 eV, and 3.5 eV as predicted by the theory. We also took some room-temperature spectra at the  $\bar{L}$  point with energy resolution of 40 meV and an angular resolution of  $\pm 0.4^\circ$ . We were still not able to resolve the fourth state. The reason for our inability to resolve the two deeper surface states at  $\bar{L}$  is most likely due to the fact that the widths are larger than the peak separation. Calculations predict a difference of 100 meV between the binding energies of the third and the fourth surface states at  $\bar{L}$  and the experimentally observed width is about 250 meV. The other small but notable discrepancy between the experimental and calculated results is the binding energy of the uppermost surface-state branch along  $\bar{\Gamma}$ - $\bar{L}$ . Calculations predict the minimum binding energy of this state to be 0.7 eV whereas the experimental value is 0.5 eV. Apart from these differences the agreement between the theory and the experiment is quite good.

## V. SURFACE ELECTRONIC BAND STRUCTURE: THEORY

As one can appreciate from Fig. 3, the present calculation gives more surface states for Be(10 $\bar{1}$ 0) than the previous theoretical studies.<sup>6,7</sup> It is explained by the fact that we now use a significantly thicker film<sup>6</sup> and a slightly less severe criterion for the definition of surface states.<sup>7</sup> In particular, we ascribe to surface states all electron states which are localized in the first four atomic layers and decay rapidly into the bulk. This criterion was also used to obtain theoretically all the surface states observed experimentally on Be(0001).<sup>3</sup> An occupied surface state with a binding energy of 3.98 eV is obtained in the symmetry gap at  $\bar{\Gamma}$ .<sup>27</sup> This is a typical dangling-bond state of the  $s$ - $p_z$  symmetry. In the vicinity of

TABLE I. Experimental and calculated surface-state binding energies (in eV) at the symmetry points indicated in column 1.

	Experiment		Theory	
	Reference 7	Present work	Reference 7	Present work
$\bar{\Gamma}$	4.05	$4.07 \pm 0.04$	3.95	3.98
$\bar{A}$	0.33	$0.416 \pm 0.02$	0.4	0.46
$\bar{L}$	2.7	$2.73 \pm 0.04$	2.6	2.71
		$2.45 \pm 0.03$	2.5	2.4
		$2.80 \pm 0.03$	2.85	2.8
		$3.40 \pm 0.05$		3.4
				3.5
$\bar{M}$	3.6	$3.47 \pm 0.05$	3.35	3.3
		$4.90 \pm 0.06$		4.8
$\bar{\Gamma}$ - $\bar{L}$ midpoint		$0.50 \pm 0.04$		0.7

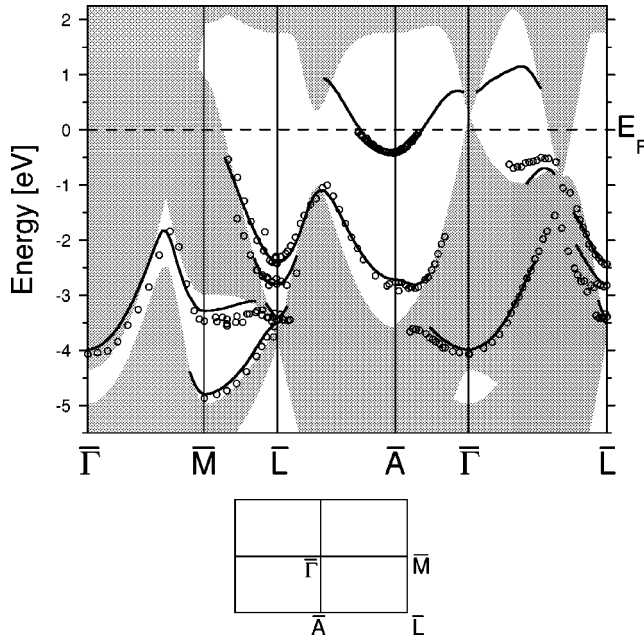


FIG. 3. Surface band structure of Be( $10\bar{1}0$ ) along the symmetry directions. The open circles are the experimental points and the solid lines are from the calculations. The grey background is the evaluated projection of the bulk band structure. The surface Brillouin zone is shown at the bottom.

the  $\bar{M}$  point the calculation gives two surface states in agreement with the experiments. The upper state with binding energy of 3.3 eV has  $p_x$  symmetry. A charge-density maximum of this state is located between the first and second atomic layers. In contrast to previous studies<sup>6,7</sup> we find in the present calculation one more surface state at  $\bar{M}$  with binding energy of 4.8 eV. This state has clear surface character and a maximum of its charge density is at the third atomic layer. It is also characterized by  $p_x$  symmetry. At the  $\bar{L}$  point, as mentioned above, we obtain four occupied surface states. The two upper surface states found also in Refs. 6 and 7 are mainly localized in the vicinity of the two outer atomic layers<sup>6</sup> while the two lower states, first obtained in the present study, have the charge-density maximum localized between the third and fourth atomic layers. All of these states are of  $p_x, p_y$  symmetry. To our knowledge no other metallic surface has four occupied surface states in a single gap. As in Refs. 6 and 7 the present calculation gives two occupied surface states at the  $\bar{A}$  point. The upper surface state has a binding energy of 0.46 eV which is in agreement with other experimental and theoretical data.<sup>7,20</sup> This state is characterized by  $s-p_z$  symmetry. The lower surface state has a binding energy of 2.7 eV and the orbital composition of the state is determined by a  $p_y$  contribution. In the  $\bar{A}-\bar{\Gamma}$  direction this state loses its surface character just beyond the energy gap.

## VI. ELECTRON-ELECTRON CONTRIBUTION TO THE INVERSE LIFETIME: THEORY

The  $\bar{A}$  shallow surface state being located in the middle of the energy gap is characterized by  $s-p_z$  symmetry. It is

known that the charge density of the  $s-p_z$  surface states on metal surfaces have a relatively small variation in the plane parallel to the surface.<sup>3,6,28–30</sup> These states can therefore be treated with reasonable accuracy by using a model potential that varies in the  $z$  direction perpendicular to the surface and is constant in the plane parallel to the surface. In the present calculations of the inverse lifetime (decay rate) of the surface-state hole we use a model potential proposed in Ref. 31 that contains four independent parameters. Two of these parameters reproduce the energy-gap width and position. The other two reproduce the binding energy of the surface state and the first image-potential state at the  $\bar{\Gamma}$  point. It was shown that this potential gives surface and image state wave functions that are in good agreement with those obtained from *ab initio* calculations.<sup>31–34</sup> The evaluated decay rate of the  $s-p_z$  surface-state hole on Be(0001) and on the (111) noble-metal surfaces was found to be in good agreement with recent scanning tunneling spectroscopy and photoemission measurements.<sup>34–36</sup>

Here we construct the model potential that accurately describes the electronic structure details at the  $\bar{A}$  point which are important for the description of the hole dynamics at the  $\bar{A}$  point. The first three details that the model potential reproduces are the width and position of the energy gap at  $\bar{A}$  obtained from our *ab initio* calculation of the projection of bulk electron states and the measured binding energy of 0.415 eV of the shallow surface state. The fourth independent parameter is used to fix the image-plane position at 2.2 a.u. beyond the surface-atomic layer. A similar position was also obtained for the image plane on the close-packed Be(0001) surface. We do not include in the description of the electronic structure the  $\bar{A}$  lower surface state since this state does not contribute to the decay rate of the shallow state hole. In contrast to previously studied metal surfaces<sup>31–36</sup> with only one interlayer spacing parameter, the Be( $10\bar{1}0$ ) slab has two interlayer spacing parameters,  $d_1$  and  $d_2$  with  $d_2 = 2d_1$ . In order to avoid this complication we chose a single interlayer spacing value which enables us to reproduce the bulk electron-density parameter  $r_s = 1.87$  a.u. By using the eigenvalues and eigenfunctions of the model potential, we performed the self-consistent calculations of the screened Coulomb interaction, the self-energy, and, finally, the  $\bar{A}$  surface state decay rate along the lines of Refs. 32–34. The quasiparticle self-energy,  $\Sigma$ , was computed with the *GW* approximation of many-body theory,<sup>37,38</sup> retaining the first term in the series expansion of  $\Sigma$  in terms of the screened Coulomb interaction  $W$ . We also replace the full Green function  $G$  by the noninteracting Green function. In order to take into account the effect of the surface corrugation on the inverse lifetime of the  $\bar{A}$  surface state hole we use the experimental effective mass  $m^* = 1.37$  of the surface state averaged over two symmetry directions,  $\bar{A}-\bar{\Gamma}$  and  $\bar{A}-\bar{L}$ . With this the self-energy calculation gives  $\tau^{-1} = 53$  meV. This includes all the *interband* transitions from bulk states as well as the *intra-band* transitions within the surface-state band. The *intra-band* transitions completely dominate the decay rate giving 52

meV and the *interband* transitions account for only 2% (1 meV) of the full  $\tau^{-1}$ .

These results are comparable with those found for the surface state at the  $\bar{\Gamma}$  point on Be(0001) (Refs. 35 and 36) and on the (111) noble-metal surfaces,<sup>34,36</sup> where the *intra*-band transitions account for  $\sim 85\%$  of the full decay rate. In contrast to Be(10 $\bar{1}$ 0), on these surfaces the  $\bar{\Gamma}$  surface state is located at the bottom of the energy gap not far from the lower energy-gap edge. Such a position of the surface state leads to two effects: (1) increasing the bulk states contribution through the smaller momentum transfer that corresponds to the *interband* transitions, and (2) decreasing the surface-state contribution (*intra*band transitions) through the smaller weight of the surface state in a vacuum region where the imaginary part of the screened Coulomb interaction,  $\text{Im } W$ , has a maximum amplitude.<sup>34</sup> For the particular case of the Cu(111) surface on which the surface state at  $\bar{\Gamma}$  has a very similar binding energy<sup>34</sup> of 0.445 eV,  $\tau_{Cu}^{-1}$  is smaller than  $\tau_{Be}^{-1}$  by factor of 2 [if we do not take into account the *d*-screening effect for Cu(111)]. Due to the  $\bar{A}$  shallow surface state position in the middle of the gap this state forms a well-defined two-dimensional (2D) electron gas. For comparison with our  $\tau^{-1} = 53$  meV value we also calculated the decay rate of this surface state by using an asymptotic formula derived within the self-energy formalism for a 2D degenerate electron-gas model (DEGM).<sup>39,40</sup> The 2D decay rate obtained for a binding energy of 0.415 eV is  $\tau_{2D}^{-1} = 125$  meV. This is substantially larger than our value of 53 meV. This difference is a direct reflection of the absence of the underlying bulk states in the 2D DEGM that strongly limits the screening of the electron-electron interaction. On the other hand, the evaluation of  $\tau^{-1}$  in the 3D DEGM (Ref. 41) gives  $\tau_{3D}^{-1} = 2$  meV which is significantly smaller than our *intra*band contribution of 52 meV but slightly larger than the *interband* one. We attribute the first result to the absence of surface states in the 3D DEGM (assumes only 3D bulk transitions and neglects band-structure effects) whereas the latter is a direct consequence of the absence of a surface energy gap in the 3D DEGM.

## VII. TEMPERATURE-DEPENDENT STUDY OF $\bar{A}$ SURFACE STATE: EXPERIMENT

Angle-resolved photoemission is a straightforward tool to measure lifetimes of two-dimensional electronic states. Under proper conditions the width obtained by angle-resolved photoemission from a valence-band state with negligible dispersion in  $k_{\perp}$  is equal to  $\hbar/\tau$ . The contribution to the width comes from electron-electron, electron-phonon, and electron-impurity interactions. It has been shown that the electron-phonon contribution to the width can be obtained from a temperature-dependent study of the width.<sup>42</sup> However it is not straightforward to separate the electron-electron and electron-impurity contributions. The electron-impurity contribution shows up in two ways: the first is the inherent contribution to the lifetime and the second is an artifact introduced by the  $E$  vs  $k_{\parallel}$  dispersion.<sup>42</sup> If one works in the region where  $\partial E/\partial k_{\parallel} = 0$ , the artifact impurity contribution is zero

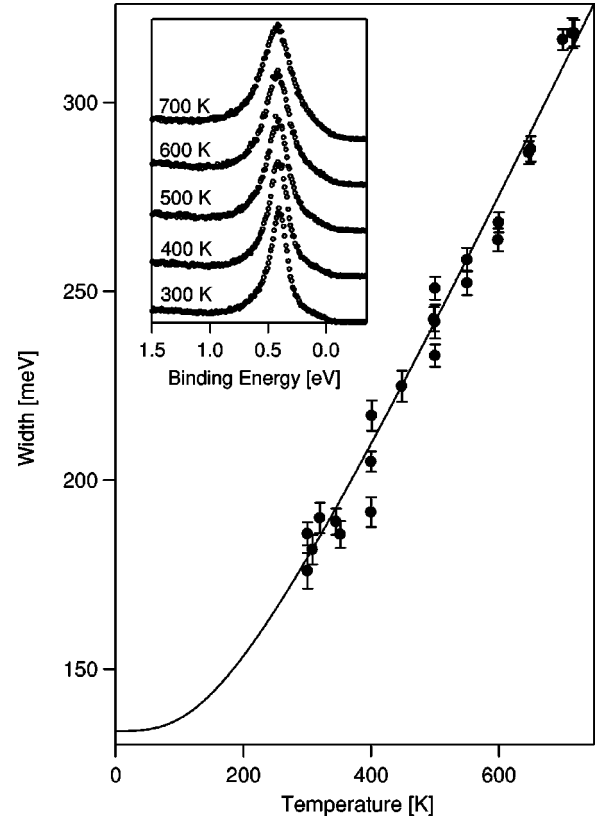


FIG. 4. The shallow  $\bar{A}$  surface state linewidth versus temperature. The inset shows surface-state spectra at various temperatures. The hole momentum is  $0.0 \text{ \AA}^{-1}$  with respect to  $\bar{A}$ . The photon energy is 21.2 eV. The energy resolution is 35 meV and the angular resolution is  $\pm 0.4^\circ$ . The filled circles are the widths obtained by fitting spectra similar to the ones shown in the inset using a Lorentzian plus a linear background times a Fermi function. The line is a fit using Eq. (1) with the Debye model for phonons. Note: The intercept on the ordinate is a sum contribution from the zero-temperature *e-ph* interaction (84 meV) and the constant  $C$  ( $48 \pm 8$  meV) of Eq. (1).

to first order. Our experiments were performed on the shallow surface state at  $\bar{A}$  where this condition is satisfied. To extract the electron-electron contribution, we compare the phonon contribution subtracted width to our model potential calculations.

The  $\bar{A}$  shallow surface state spectra recorded at various temperatures are shown in the inset of Fig. 4. The photon energy used was 21.2 eV and the energy and angular resolution were 35 meV and  $\pm 0.4^\circ$ , respectively. Figure 4 shows the width versus temperature obtained from these and other similar spectra. The electron-phonon contribution to the width and the residual width is obtained in the following way. The electron-phonon contribution to the lifetime at any temperature is given by the formula<sup>43</sup>

$$\begin{aligned}
 W_{ep}(\omega) &= \hbar/\tau_{ep}(\omega) \\
 &= 2\pi\hbar \int_0^{\omega_m} d\omega' \alpha^2 F(\omega') [1 - f(\omega - \omega') + 2n(\omega') \\
 &\quad + f(\omega + \omega')] + C,
 \end{aligned} \tag{1}$$

where  $\alpha^2 F(\omega)$  is the Eliashberg coupling function,  $\omega_m$  is the maximum phonon frequency,  $f(\omega)$  and  $n(\omega)$  are the Fermi and Bose-Einstein distributions, and  $C$  is a constant. We use a simple 3D Debye model with  $\alpha^2 F(\omega) = b(\omega/\omega_m)^2$ , where  $b = 2 \int_0^{\omega_m} d\omega \alpha^2 F(\omega)/\omega$ . Note that for energies close to  $E_F$ ,  $b$  coincides with the electron-phonon mass enhancement parameter  $\lambda$ . We took  $\hbar\omega_m = 60$  meV. By fitting the experimental width versus temperature to the above equation, we obtain  $b = 0.665 \pm 0.03$  and  $C = 51 \pm 8$  meV. With this  $b$  the 3D Debye model gives  $\tau_{e-ph}^{-1} = 83.5$  meV. In order to study the surface effects in the  $e-ph$  interaction we have calculated  $\tau_{e-ph}^{-1}$  for the 2D Debye model with the same  $b$  and  $\lambda$ . The obtained  $\tau_{e-ph}^{-1} = 80$  meV shows only slight deviation from the 3D  $\tau_{e-ph}^{-1}$  value. This result indicates that the  $e-ph$  contribution is not very sensitive to the dimensionality and phonon distribution function. The origin of this stability is that the  $\bar{A}$  surface state energy lies well below the maximum phonon energy and that the phonon spectrum enters Eq. (1) in integral form. So, the 3D Debye model is not expected to be a significant source of error. Earlier studies of the temperature dependence of the width on the same surface state at a binding energy of 200 meV reported  $b = 0.672 \pm 0.027$  along the  $\bar{A}-\bar{L}$  direction, and  $b = 0.642 \pm 0.031$  along the  $\bar{A}-\bar{\Gamma}$  direction.<sup>20</sup> Within the experimental error bars, the values of  $b$  are similar. In Ref. 20 a correction factor had to be applied to take care of the variation of  $k_{\parallel}$  within the peak which makes the peaks appear broader by a factor  $[1 - (\partial E / \partial k_{\parallel})(m/\hbar^2)(\sin^2 \theta/k_{\parallel})]^{-1}$ , where  $m$  is the free-electron mass. Since the present study is done at a point where  $\partial E / \partial k_{\parallel} = 0$ , the correction factor need not be applied and quite clearly within error bars our results agree with it. Though this is a trivial theoretical result, it is interesting to see experimental proof for it. As mentioned above the calculations give the  $e-e$  contribution to be 53 meV for the surface state at  $\bar{A}$ . Experimentally we obtain the phonon contribution (84 meV) removed width to be  $51 \pm 8$  meV which is similar to the theoretical value. One should however bear in mind that the experimentally determined width contains both the electron-electron and electron-impurity contributions and it is difficult to experimentally separate these two contributions. If we assume the impurity mean free path to be similar to that on Be(0001) and noble-metal surfaces (about 50 Å), one would expect an impurity contribution of about 10–15

meV. So the experimental  $e-e$  contribution is expected to be around 40 meV which is smaller by  $\sim 20\%$  than our theoretical result. There are two points that can explain this discrepancy. Our recent *ab initio* calculations show that the model potential evaluations give the inverse lifetime of a hole in the  $s-p_z$  surface state to be 10% larger than first-principles calculations.<sup>35,44</sup> On the other hand a model that we use to estimate the  $e-ph$  contribution is based on a simple bulk description of phonon modes (the Debye model) and electron states. Recent calculations for noble-metal surfaces (111) that take explicitly into account the surface phonon modes and accurate wave function of a surface state of interest give a slightly smaller (within 10%)  $e-ph$  contribution compared to the Debye model.<sup>45</sup> Therefore, one can expect that the more accurate description of  $\tau_{e-ph}^{-1}$  for the  $\bar{A}$  shallow surface state will decrease the Debye model value of  $\tau_{e-ph}^{-1}$  and will increase, respectively, the experimental  $\tau_{e-e}^{-1}$  to better agreement with the theoretical value.

## VIII. CONCLUSIONS

In conclusion we have presented the electronic band structure of the Be(10 $\bar{1}$ 0) surface experimentally determined by angle-resolved photoemission and calculated by using density-functional theory. The experimental results agree well with the calculations, except for the fact that we were able to resolve three surface states in the gap at  $\bar{L}$ , instead of four as predicted by the calculations. From the temperature-dependent study of the  $\bar{A}$  shallow surface state we determined phonon contribution subtracted width to be  $51 \pm 8$  meV. This compares fairly well with the calculated contribution of 53 meV for the electron-electron interaction to the width.

## ACKNOWLEDGMENTS

We are grateful for the support of MAX-lab staff and the financial support from the Swedish Natural Research Council. This work was partially supported by the University of the Basque Country, the Basque Hezkuntza, Unibertsitate eta Ikerketa Saila, and the Spanish Ministerio de Educación y Cultura. Partial support from the Max Planck Research Award funds is gratefully acknowledged.

<sup>1</sup>U.O. Karlsson, S.A. Flodström, R. Engelhardt, W. Gädeke, and E.E. Koch, *Solid State Commun.* **49**, 711 (1984).

<sup>2</sup>R.A. Bartynski, E. Jensen, T. Gustafsson, and E.W. Plummer, *Phys. Rev. B* **32**, 1921 (1985).

<sup>3</sup>E.V. Chulkov, V.M. Silkin, and E.N. Shirykalov, *Surf. Sci.* **188**, 287 (1987).

<sup>4</sup>P.J. Feibelman, *Phys. Rev. B* **46**, 2532 (1992).

<sup>5</sup>N.A. Holzwarth and Y. Zheng, *Phys. Rev. B* **51**, 13 653 (1995).

<sup>6</sup>V.M. Silkin and E.V. Chulkov, *Fiz. Tverd. Tela (St. Petersburg)* **37**, 2795 (1995) [*Phys. Solid State* **37**, 1540 (1995)].

<sup>7</sup>Ph. Hofmann, R. Stumpf, V.M. Silkin, E.V. Chulkov, and E.W.

Plummer, *Surf. Sci.* **355**, L278 (1996).

<sup>8</sup>Ph. Hofmann, K. Pohl, R. Stumpf, and E.W. Plummer, *Phys. Rev. B* **53**, 13 715 (1996).

<sup>9</sup>P.T. Sprunger, L. Petersen, E.W. Plummer, E. Laegsgaard, and F. Besenbacher, *Science* **275**, 1764 (1997).

<sup>10</sup>Ph. Hofmann, B.G. Briner, M. Doering, H.-P. Rust, E.W. Plummer, and A.M. Bradshaw, *Phys. Rev. Lett.* **79**, 265 (1997).

<sup>11</sup>L.I. Johansson, H.I. Johansson, J.N. Andersen, E. Lundgren, and R. Nyholm, *Phys. Rev. Lett.* **71**, 2453 (1993).

<sup>12</sup>H.I.P. Johansson, L.I. Johansson, J.N. Andersen, E. Lundgren, and R. Nyholm, *Phys. Rev. B* **49**, 17 460 (1994).

- <sup>13</sup>P.J. Feibelman and R. Stumpf, Phys. Rev. B **50**, 17 480 (1994).
- <sup>14</sup>L.I. Johansson, P.-A. Glans, and T. Balasubramanian, Phys. Rev. B **58**, 3621 (1998).
- <sup>15</sup>S. Lizzit, K. Pohl, A. Baraldi, G. Comelli, V. Fritzche, E.W. Plummer, R. Stumpf, and Ph. Hofmann, Phys. Rev. Lett. **81**, 3271 (1998).
- <sup>16</sup>T. Balasubramanian, E. Jensen, X.L. Wu, and S.L. Hulbert, Phys. Rev. B **57**, 6866 (1998).
- <sup>17</sup>M. Hengsberger, D. Purdie, P. Segovia, M. Garnier, and Y. Baer, Phys. Rev. Lett. **83**, 592 (1999).
- <sup>18</sup>M. Hengsberger, R. Frésard, D. Purdie, P. Segovia, and Y. Baer, Phys. Rev. B **60**, 10 796 (1999).
- <sup>19</sup>S. LaShell, E. Jensen, and T. Balasubramanian, Phys. Rev. B **61**, 2371 (2000).
- <sup>20</sup>T. Balasubramanian, P.-A. Glans, and L.I. Johansson, Phys. Rev. B **61**, 12 709 (2000).
- <sup>21</sup>V.M. Silkin, E.V. Chulkov, and P.M. Echenique, Phys. Rev. B **60**, 7820 (1999).
- <sup>22</sup>B.N. Jensen, S.M. Butorin, T. Kaurila, R. Nyholm, and L.I. Johansson, Nucl. Instrum. Methods Phys. Res. A **394**, 243 (1997).
- <sup>23</sup>P. Butcher and R.I.G. Uhrberg, Phys. World **Sept. 1995**, 48 (1995).
- <sup>24</sup>L. Hedin and B.I. Lundqvist, J. Phys. C **4**, 2062 (1971).
- <sup>25</sup>V.M. Silkin, E.V. Chulkov, I.Yu. Sklyadneva, and V.E. Panin, Sov. Phys. J. **27**, 762 (1984).
- <sup>26</sup>E.V. Chulkov, V.M. Silkin, and E.N. Shirykalov, Phys. Met. Metallogr. **64**, 1 (1987).
- <sup>27</sup>V.M. Silkin, E.V. Chulkov, and P.M. Echenique, Fiz. Tverd. Tela (St. Petersburg) **41**, 935 (1999) [Phys. Solid State **41**, 848 (1999)].
- <sup>28</sup>L. Ley, G.P. Kerker, and N. Martensson, Phys. Rev. B **23**, 2710 (1981).
- <sup>29</sup>J. Inglesfield and G.A. Benesh, Phys. Rev. B **37**, 6682 (1988).
- <sup>30</sup>E.V. Chulkov and V.M. Silkin, Surf. Sci. **215**, 385 (1989).
- <sup>31</sup>E.V. Chulkov, V.M. Silkin, and P.M. Echenique, Surf. Sci. **391**, L1217 (1997); **437**, 330 (1999).
- <sup>32</sup>E.V. Chulkov, I. Sarria, V.M. Silkin, J.M. Pitarke, and P.M. Echenique, Phys. Rev. Lett. **80**, 4947 (1998).
- <sup>33</sup>I. Sarria, J. Osmá, E.V. Chulkov, J.M. Pitarke, and P.M. Echenique, Phys. Rev. B **60**, 11 795 (1999).
- <sup>34</sup>J. Kliewer, R. Berndt, E.V. Chulkov, V.M. Silkin, P.M. Echenique, and S. Crampin, Science **288**, 1399 (2000).
- <sup>35</sup>V. M. Silkin, T. Balasubramanian, E. V. Chulkov, A. Rubio, and P. M. Echenique, Phys. Rev. B **64**, 085334 (2001).
- <sup>36</sup>E.V. Chulkov, V.M. Silkin, and P.M. Echenique, Surf. Sci. **454-456**, 458 (2000).
- <sup>37</sup>L. Hedin and S. Lundqvist, Solid State Phys. **23**, 1 (1969).
- <sup>38</sup>P.M. Echenique, J.M. Pitarke, E.V. Chulkov, and A. Rubio, Chem. Phys. **251**, 1 (2000).
- <sup>39</sup>A.V. Chaplik, Zh. Éksp. Teor. Fiz. **60**, 1845 (1971) [Sov. Phys. JETP **33**, 997 (1971)].
- <sup>40</sup>G.F. Giuliani and J.J. Quinn, Phys. Rev. B **26**, 4421 (1982).
- <sup>41</sup>J.J. Quinn, Phys. Rev. **126**, 1453 (1962).
- <sup>42</sup>B.A. McDougall, T. Balasubramanian, and E. Jensen, Phys. Rev. B **51**, 13 891 (1995).
- <sup>43</sup>G. Grimvall, *The Electron-Phonon Interaction in Metals* (North-Holland, Amsterdam, 1981).
- <sup>44</sup>V. M. Silkin, E. V. Chulkov, and P. M. Echenique (unpublished).
- <sup>45</sup>B. Hellsing, A. Eiguren, E. V. Chulkov, V. M. Silkin, and P. M. Echenique (unpublished).